NANO LETTERS

LETTER

pubs.acs.org/NanoLett

Electric Field Induced Removal of the Biexciton Binding Energy in a Single Quantum Dot

Michael E. Reimer,*[,†,§] Maarten P. van Kouwen,[†,§] Anne W. Hidma,[†] Maarten H. M. van Weert,[†] Erik P. A. M. Bakkers,[†,‡] Leo P. Kouwenhoven,[†] and Val Zwiller[†]

[†]Kavli Institute of Nanoscience, Delft University of Technology, Delft, The Netherlands

[‡]Technical University of Eindhoven, Eindhoven, The Netherlands

ABSTRACT: We control the electrostatic environment of a single InAsP quantum dot in an InP nanowire with two contacts and two lateral gates positioned to an individual nanowire. We empty the quantum dot of excess charges and apply an electric field across its radial dimension. A large tuning range for the biexciton binding energy of 3 meV is obtained in a lateral electric field. At finite lateral electric field the exciton and biexciton emission overlap within their optical line width resulting in an enhancement of the observed photoluminescence intensity. The electric field dependence of the exciton and biexciton is compared to theoretical predictions and found to be in good qualitative agreement. This result is promising toward generating entangled photon pairs on demand without the requirement to remove the anisotropic exchange splitting from asymmetric quantum dots.

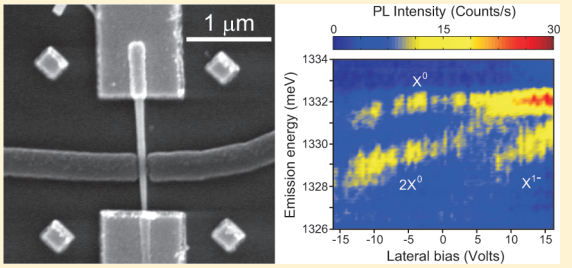

KEYWORDS: Biexciton binding energy, lateral electric field, quantum dot, nanowire, entanglement, photoluminescence, single electron charging

The development of a polarization entangled photon source on demand is a crucial requirement for applications in quantum information and quantum optics.[1,2] Semiconductor quantum dots offer the possibility to generate such entangled photon pairs on demand by the polarization of emitted photons from the biexciton−exciton radiative cascade.[3] The anisotropic exchange splitting (AES) of the intermediate exciton states in the radiative cascade, however, provides which-path information through a photon energy measurement and thereby destroys the conditions for entanglement. The which-path information can be circumvented to restore entanglement through spectral filtering,[4] optical field tuning,[5] or AES removal.[6−8] The successful removal of the AES has been achieved by quantum dot size and composition engineering,[6−8] growth of highly symmetric site-selected quantum dots,[9] thermal annealing,[10] and the application of an in-plane magnetic[11] or electric field.[12−14] More recently, it was predicted that quantum dots in nanowires emit entangled photon pairs due to their symmetry and thus vanishing AES;[15] however, we have observed a nonzero AES in previous optical studies of single quantum dots in nanowires.[16] A proposal that circumvents this requirement and produces entangled photon pairs even in the presence of nonzero AES relies on tuning the biexciton binding energy to zero.[17−19] In such a scheme, the photons are entangled provided that the timing information of the exciton and biexciton is erased in the measurement setup.[20] Experimental methods to remove the biexciton binding energy to zero include the use of lateral strain[21] or local lateral electric fields.[17,18] However, in these schemes, the binding energy of the biexciton was tuned over a very small energy range, approximately 600 μeV in the case of lateral strain,[21] and 200 μeV in the case of local lateral electric fields.[17,18]

In the work presented here, we demonstrate the removal of the biexciton binding energy of a single InAsP quantum dot embedded in an InP nanowire by a lateral electric field. In contrast to previous work,[14,17,18,21] we show that the binding energy of the biexciton can be tuned over a large energy range (~3 meV). Since typical binding energies of the biexciton are within the energy range of 3 meV,[22] the observed tuning range that we demonstrate allows for biexciton binding energy removal on each quantum dot desirable in constructing arrays of entangled photon pair sources for quantum information applications. The method we utilize has the added benefit that it can be performed dynamically at high frequencies, postgrowth and on-chip by simply applying a voltage. Finally, similar to previous reports[23] we demonstrate precise control of the excess charges in the quantum dot by an applied electric field along the nanowire elongation axis. Such control allows us to empty the quantum dot of excess charges and observe neutral excitons and biexcitons necessary for the present experiments.

The device details used in the present experiments are introduced in Figure 1a and Figure 1b. In Figure 1a, a scanning electron micrograph (SEM) of a single contacted InP nanowire with an embedded InAsP quantum dot is presented. In Figure 1b, the device geometry and electrical circuitry are presented schematically. The two lateral gates in the vicinity of the nanowire and two Schottky contacts along the nanowire allow for the control of the electrostatic environment in the quantum dot and nanowire. The two Ti/Al Schottky contacts (source, V_s, and drain, V_d) enable an

Received: October 25, 2010
Revised: December 16, 2010
Published: January 12, 2011

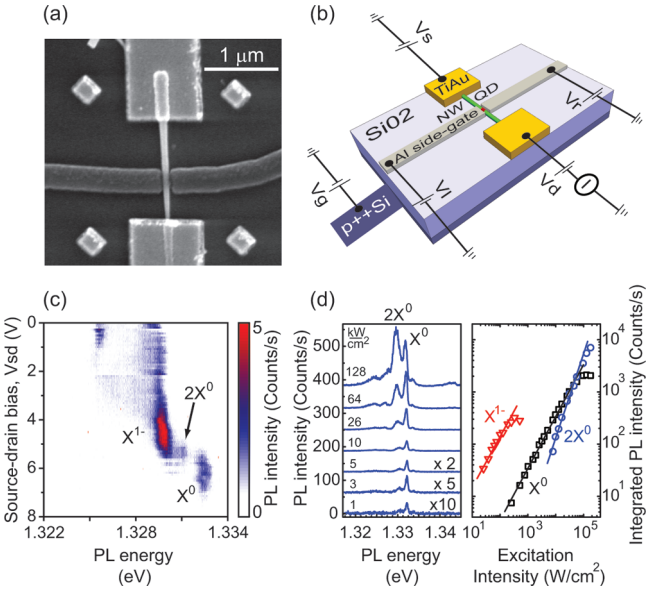

Figure 1. (a) SEM micrograph of single contacted nanowire with embedded quantum dot. (b) Circuit schematics of device: V_s, source; V_d, drain; V_l, left side-gate; V_r, right side-gate; V_g, back-gate. (c) Typical electron charging diagram of single InAsP quantum dot in an InP nanowire at low temperature (4.2 K) and excitation close to the band-edge of InP (1.46 eV). $V_g = V_l = V_r = 0$ V. (d) Left: PL spectra under increasing excitation power at $V_{sd} = 5.2$ V and excitation energy of 2.33 eV. The spectra are offset along the y axis for clarity. Right: fitted integrated PL intensity from left panel (open symbols) vs excitation intensity. Solid lines are fits to data for exciton (slope = 1) and biexciton (slope = 1.6). For comparison, the integrated PL intensity of X^{1-} at $V_{sd} = 4$ V is also shown (slope = 1).

electric field to be applied along the nanowire elongation axis, which precisely controls the number of electrons in the quantum dot.[23] The lateral gates (left, V_l, and right, V_r), which are aligned to the middle of the nanowire are used to induce an electric field across the radial dimension of the quantum dot. See Methods section for further details of the dot growth in a nanowire and device fabrication. The separation of the two lateral gates (Ti/Al) is ∼160 nm. To ensure minimal potential changes at the quantum dot position due to parasitic gating effects, in the following, we apply $V_s = -V_d = V_{sd}/2$ for the electric field along the nanowire axis and $V_l = -V_r$ to induce a lateral electric field across the quantum dot. Assuming the nanowire diameter is $d/2$ (obtained from the SEM image of Figure 1a), the lateral electric field, F, inside the nanowire is defined as $F = (V_r - V_l)/([2\varepsilon - 1]d)$. In this expression, ε is the dielectric constant of the nanowire and d is the separation of the two lateral gates. Using the dielectric constant of InP ($\varepsilon = 12.4$), we estimate an applied lateral bias of 1 V to be $F \sim 2.6$ kV/cm.

The effect of an applied electric field along the nanowire elongation axis (source−drain bias, V_{sd}) on the photoluminescence (PL) is presented in Figure 1c. In these electric field measurements, we use a low excitation power to avoid screening of the applied electric field by the optically excited carriers. Thus, on average we observe singly charged exciton complexes in the PL emission spectra of Figure 1c. Increasing V_{sd} results in subsequent discharging events corresponding to discrete energy steps in the optical emission. At large V_{sd} (>6 V), a single peak is observed at 1.3320 eV and is identified as the neutral exciton, X^0, involving electron−hole recombination in the quantum dot s-shell. The

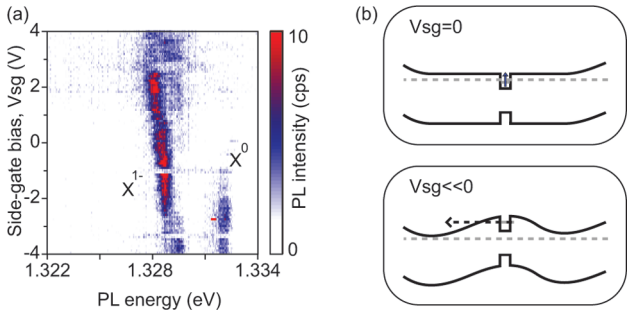

Figure 2. (a) Low temperature (4.2 K) single dot PL as a function of side-gate bias. Laser excitation is performed resonantly in the quantum dot d-shell (1.37 eV); $V_{sd} = 5.2$ V. (b) Schematic view of 1D bandstructure along the nanowire at $V_{sg} = 0$ V (top) and $V_{sg} \ll 0$ V (bottom), which corresponds to a single resident electron and empty quantum dot, respectively.

identification of X^0 was determined by resonant photocurrent experiments in earlier work.[23] Decreasing V_{sd} to ≃6 V the singly charged exciton, X^{1-}, appears in the optical spectrum as X^0 quenches. In this particular quantum dot, addition of an extra electron shifts the X^{1-} PL emission energy to 2.6 meV below the X^0 emission. This shift to lower energy is due to the strong electron−hole Coulomb interactions present in quantum dots involving exciton recombination in the presence of an additional resident electron and is similar to previously reported X^{1-} binding energies of InAsP dots embedded in InP nanowires.[23] In a small bias range, a peak at 1.3305 eV can be observed between the X^{1-} and X^0 emission lines. We attribute this peak as the biexciton ($2X^0$) since during the optical excitation process an optically excited hole may be captured to neutralize X^{1-}, thus resulting in $2X^0$ emission.[24] Such behavior has been observed before for InGaAs quantum dots embedded in GaAs when the tunneling barrier between the back n-doped contact and quantum dot layer is relatively large (∼40 nm).[24] In contrast, when the back contact to quantum dot layer separation is reduced, the biexciton is not observed at low excitation powers.[24] Confirmation of our assignment for the $2X^0$ peak is corroborated by the power-dependent PL shown in Figure 1d at $V_{sd} = 5.2$ V. As a function of increasing excitation power, the integrated PL intensity for X^0 exhibits a linear power dependence whereas a superlinear power dependence is observed for $2X^0$ (slope ∼1.6). More extensive optical studies for single quantum dots in individual nanowires can be found in refs 16, 23, and 25.

For comparison, we also show the integrated PL intensity of X^{1-} in Figure 1d taken at a lower source−drain bias ($V_{sd} = 4$ V). The observed linearity of the X^{1-} power dependence indicates deterministic control of the electron charge state confined in the quantum dot through tunneling events in the initial and final state influenced by an applied electric field along the nanowire.[23] This deterministic control of the electron charge state allows us to prepare neutral excitons and biexcitons necessary for the experiments to be presented subsequently. We note, however, that the quantum dot suffers from charge fluctuations in its environment most likely caused by surface states or ionized donors in the nanowire. These charge fluctuations in the environment result in a temporary change in the charge state configuration that occurs during the PL integration time in the order of seconds (see Figure 1c). At larger V_{sd}, the quantum dot emission becomes more stable compared to lower V_{sd} as surface states in the

dx.doi.org/10.1021/nl1037424 |Nano Lett. 2011, 11, 645–650

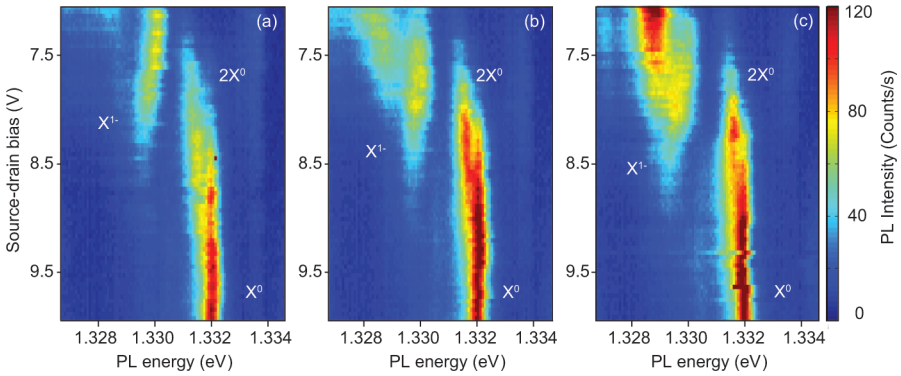

Figure 3. Low temperature (4.2 K) source−drain bias sweeps at V_{lat} of (a) 0, (b) 6, and (c) 12 V under d-shell excitation (1.37 eV). The exciton and biexciton splitting is no longer resolved in (c) for V_{lat} = 12 V.

nanowire are emptied due to the high electric field. This charge stability is evident in the power-dependent spectra of Figure 1d since there are no observed fluctuations in intensity for the exciton and biexciton emission.

We demonstrate further control of the electrostatic environment for the quantum dot in a nanowire by applying an equal potential to both lateral gates ($V_{sg} = V_l = V_r$). In Figure 2a the single quantum dot PL as a function of equal potential applied to both lateral gates is presented. For this voltage sweep the quantum dot is first biased to X^{1-} with V_{sd} = 5.2 V and V_{sg} = 0 V (see Figure 1c). As V_{sg} is tuned from +4 to −4 V, an increase in energy for the X^{1-} emission of ∼1.5 meV is observed. The shift to higher energy is attributed to both an increase in electron−electron repulsion as negative V_{sg} pushes the two electrons closer together and a decrease in electron−hole Coulomb repulsion as the holes are attracted closer to the edge of the wire. In contrast, the X^0 emission exhibits no energy shift. In this case, the constant X^0 emission indicates that the reduction in electron−hole Coulomb attraction compensates the single particle Stark shift.[18] In addition to affecting Coulomb interactions in the quantum dot, operation of the lateral gates at equal potential allows the electrochemical potential of the nanowire to be tuned locally, which strongly affects the confined charge. See Figure 2b for a schematic view of the band structure for V_{sg} = 0 V and $V_{sg} \ll 0$ V and corresponding charge states. The effect of modifying the electrochemical potential is evident at $V_{sg} \sim -1$ V where the charge state changes from predominantly X^{1-} to X^0.

In the following, we manipulate the applied biases on the two contacts and two lateral gates that surround the quantum dot to engineer[19] the exciton and biexciton splitting to zero. The effect of the applied lateral electric field on the quantum dot PL emission is presented in Figure 3 and Figure 4. In these experiments $V_l = -V_r$ and the lateral gate potential is defined as $V_{lat} = V_r - V_l$. Moreover, the excitation power is increased such that the exciton and biexciton emission peaks are equal in intensity. Since the power is increased to observe biexciton emission, laser excitation resonant in the quantum dot d-shell is used in order to avoid screening of the applied electric field due to optically excited carriers in the nanowire. In Figure 3, three different source−drain bias sweeps for a small voltage range are shown at V_{lat} = 0 V, V_{lat} = 6 V, and V_{lat} = 12 V in (a), (b), and (c), respectively. At zero applied lateral electric field (Figure 3a, V_{lat} = 0 V), the exciton and biexciton transitions are well separated in energy. As V_{lat} increases the reduction in the exciton−biexciton splitting is clearly observed. In Figure 3c (V_{lat}=12 V), there is no longer a distinction between the exciton and biexciton emission peaks.

To determine the applied lateral electric field at which the biexciton binding energy is tuned to zero, we now vary V_{lat} at a fixed source−drain bias where we observe both the exciton and biexciton simultaneously with equal emission intensity and at a higher spectral resolution (30 μeV). The results of the PL emission for X^0 and $2X^0$ as a function of lateral bias at V_{sd} = 5.2 V are presented in Figure 4a. The difference between the exciton and biexciton emission is known as the biexciton binding energy, $\Delta XX = E_{X^0} - E_{2X^0}$. At V_{lat} = 0 V, ΔXX is ∼2 meV. Here, ΔXX is mainly determined by the competition between Coulomb repulsion among electrons (V_{ee}) and holes (V_{hh}), Coulomb electron−hole attraction (V_{eh}), and correlation corrections (ΔE_{corr}) due to higher lying states confined in the quantum dot.[19] At zero electric field, the biexciton can appear either at higher or lower emission energy depending on the dot size.[22] In cases where ΔXX is positive, the biexciton emission can be engineered to cross the exciton emission at finite electric field.[19] Similar behavior is observed in Figure 4a for increasing electric field (lateral bias). Before the expected crossing, X^0 exhibits a very small red shift while a strong blue shift of $2X^0$ is observed. At a finite bias of V_{lat} = 10 V, $2X^0$ merges with X^0 and the two peaks cannot be distinguished within the optical line width of the two transitions. After the expected crossing, we observe an increase in PL intensity, which suggests that the PL amplitudes of X^0 and $2X^0$ are added. Increasing the lateral bias further to V_{lat} = 16 V the exciton-biexciton splitting still cannot be resolved and $2X^0$ does not appear on the other side of X^0. Recently, such a crossing of the exciton-biexciton was observed in a macroscopic lateral electric field effect device containing an ensemble of InGaAs self-assembled quantum dots surrounded in a three-dimensional GaAs host matrix.[26] In contrast to that work, we utilize local lateral electric fields on a single quantum dot with independent control of the charge state. Of particular significance here, ΔXX is tuned by approximately 3 meV. The large tuning range that we demonstrate is promising for removal of the biexciton binding energy on an array of quantum dots without significant loss of oscillator strength of the exciton and biexciton. It should be noted, however, that there is an observed asymmetry about zero applied bias that is likely caused by the quantum dot not being in the center of the lateral gates. Such dot misalignment to the gates can lead to a small electric field component along the nanowire, which results in the strong Stark shift of X^0 and $2X^0$ to lower energies for negative lateral biases and the appearance of X^{1-} in the optical spectrum at positive lateral bias

dx.doi.org/10.1021/nl1037424 |*Nano Lett.* 2011, 11, 645–650

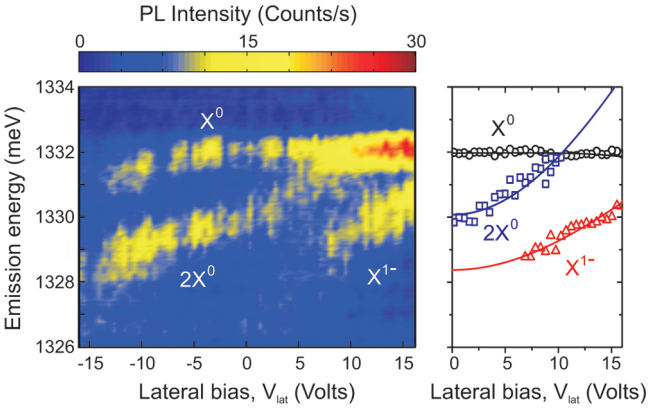

Figure 4. (a) Removal of biexciton binding energy in a lateral electric field. V_{sd} = 5.2 V; T = 4.2 K; excitation energy = 1.37 eV. (b) Solid lines are fit to peak positions of X^0, $2X^0$, and X^{1-} optical transitions in a lateral electric field from (a) for positive lateral bias using realistic system parameters for the quantum dot in a nanowire. See text for fit parameters.

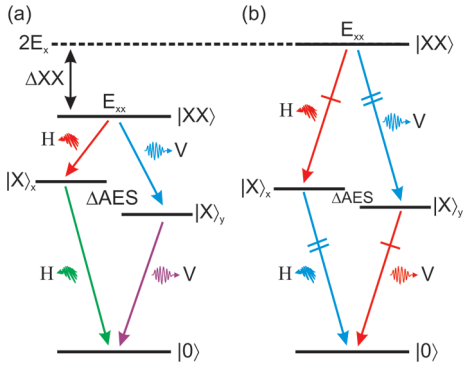

Figure 5. Concept to realize entangled photon pairs from the biexciton−exciton radiative cascade through removal of the biexciton binding energy, ΔXX. There are two possible recombination pathways from the biexciton state, $|XX\rangle$, through the intermediate exciton states, $|X\rangle_x$ and $|X\rangle_y$, to the ground state, $|0\rangle$. (a) At zero electric field, each photon emitted in the cascade has a different color in the presence of an anisotropic exchange splitting (ΔAES). (b) At finite electric field, two degenerate transitions can be identified once the biexciton binding energy has been removed, thus restoring conditions for polarization entangled photons: H, horizontal polarization; V, vertical polarization.

(V_{lat} = 7 V). Our assignment of X^{1-} is confirmed by its emission energy and dependence on electric field since it is also expected to blue shift for increasing lateral electric field.[18]

To understand the origin for removal of the biexciton binding energy observed in Figure 4a we compare peak positions of X^0, $2X^0$, and X^{1-} for positive lateral bias to calculations similar to those for Korkusinski et al.[19] These calculations are based on a full configuration-interaction method utilizing the effective mass approach and assuming a 2D parabolic potential in the radial dimension of the quantum dot.[19] Including Coulomb interactions and neglecting correlations since correlations are relatively insensitive to the applied lateral field,[19] the exciton energy $E_{X^0} = E_e + E_h - V_{eh}$, where E_e and E_h are the single particle energies for the electron and hole, respectively. As the final state of the exciton is an empty quantum dot, E_{X^0} also defines the energy of PL emission for X^0. The biexciton energy is $E_{XX} = 2E_e + 2E_h + V_{ee} + V_{hh} - 4V_{eh}$. Since the final state of the biexciton is the exciton state, the PL emission energy for the biexciton transition is $E_{2X^0} = E_{XX} - E_{X^0} = E_e + E_h + V_{ee} + V_{hh} - 3V_{eh} = E_{X^0} + (V_{ee} + V_{hh} - 2V_{eh})$. In those calculations, the exciton (first term) exhibits a very small Stark shift to lower energies with applied lateral electric field (bias) due to the competing single particle and electron−hole Coulomb interactions.[18,19] The Coulomb interactions of the same type (V_{ee} and V_{hh}) do not vary as a function of the applied field since the shell structure is not changed by the symmetry breaking introduced by the field.[19] In contrast, increasing the electric field drives the biexciton emission toward higher energies due to the field-induced electron−hole separation and corresponding exponential decrease of V_{eh}.[18,19] This strong reduction in V_{eh} with lateral electric field eventually leads to a cancelation of the interaction terms and crossing of exciton and biexciton optical transitions. Such behavior is qualitatively observed in Figure 4a at positive lateral bias where dissimilar energy shifts of exciton and biexciton result in their eventual merging at finite lateral electric field.

Taking realistic parameters for the confinement potential of our quantum dot in a nanowire and measured s-shell, p-shell splitting of 17 meV, we utilize the model of Korkusinski et al. for a 2D parabolic potential in a lateral electric field.[19] The results of the electric field dependence for the X^0, $2X^0$, and X^{1-} optical transitions for positive lateral bias are shown in Figure 4b. Excellent qualitative agreement is found between the theoretical prediction (solid lines) and experiment (open symbols) when using the following system parameters: zero field electron−hole binding energy, $V_{eh}{}^0$ = 14.5 meV; zero field biexciton binding energy Δ_{XX} = 1.9 meV; zero field X^{1-} binding energy Δ_{X1-} = 3.6 meV; confinement energy of electron, $\hbar\omega_e$ = 14.3 meV; confinement energy of hole, $\hbar\omega_h$ = 2.7 meV; electron effective mass, $m_e{}^* = 0.06m_0$; heavy-hole effective mass, $m_h{}^* = 0.55m_0$. We note here that $\hbar\omega_e$ and $\hbar\omega_h$ are the only fitting parameters. To overlap the electric field axis with the applied lateral bias in Figure 4b, we find that at the exciton−biexciton crossing of 10 V that we observe, the applied field corresponds to F = 2.8 kV/cm. At such low lateral electric fields the oscillator strength of the optical transitions of exciton and biexciton is calculated to be 94%. This overlap of electron and hole is significantly higher than electric field based methods that rely on the AES removal of the intermediate exciton states in order to produce entangled photon pairs.[12,13,18]

There is one main discrepancy between experiment and theory beyond the exciton−biexciton crossing in Figure 4. In experiment, the biexciton does not continue to strongly blue shift as the theoretical prediction suggests. Instead, we only observe a small blue shift and increase in PL intensity. Here, the intensity doubles compared to lower lateral electric field, which suggests that the exciton and biexciton indeed merge and do not cross. The merging of X^0 and $2X^0$ is possible if after the predicted crossing the two excitons forming the biexciton state are two spatially separated excitons that can therefore emit at the same energy. In this case, the electron−electron and hole−hole repulsion would be close to zero and the two independent excitons would behave similarly in an electric field once the biexciton binding energy has been removed.

The concept to realize entangled photon pairs from removal of the biexciton binding energy is shown schematically in Figure 5 by the biexciton−exciton radiative cascade.[17,19] At zero electric field and in the presence of an anisotropic exchange splitting (ΔAES) (Figure 5a), each photon emitted in the cascade emits at a different color. Thus, the recombination pathway can be distinguished and the emitted photons are classically correlated. However, tuning the biexciton binding energy to zero in a lateral electric

dx.doi.org/10.1021/nl1037424 |*Nano Lett.* 2011, 11, 645–650

field (Figure 5b) results in the degeneracy of the cross-color transitions in the cascade (i.e., $|XX\rangle \rightarrow |X\rangle_x$ and $|X\rangle_y \rightarrow |0\rangle$; $|XX\rangle \rightarrow |X\rangle_y$ and $|X\rangle_x \rightarrow |0\rangle$). In this case, the which-path information cannot be distinguished and the emitted photons are entangled in the polarization degrees of freedom, $|\Psi\rangle = 1/\sqrt{2}(|XX\rangle_V|X\rangle_V + |XX\rangle_H|X\rangle_H)$.[17,19,20] We note that to maintain the conditions of entanglement, the biexciton photon should be delayed with respect to the exciton photon in order to "erase" the timing information of emitted photons.[20]

In conclusion, we demonstrated a high level of control over the electrostatic environment for a single InAsP quantum dot embedded in an InP nanowire. We first prepared the quantum dot to be empty of excess charges by an electric field applied along the nanowire growth axis such that we observe both neutral excitons and biexcitons. We engineered the exciton−biexciton splitting for an individual quantum dot by a local lateral electric field. We showed that the biexciton binding energy can be tuned over a large energy range, from 3 meV to 0. This result is a significant step toward entangled photon pair generation on demand in the presence of AES from asymmetric quantum dots. In order to make this solution viable for quantum dots in nanowires in the future, improvements to the current PL count rates and access to polarization information of nanowire devices are necessary. Detected PL count rates of quantum dots in nanowires can be drastically improved by designing waveguiding structures[27] and polarization information can be accessed if excited and collected along the nanowire growth axis.[25] Finally, embedded dots in nanowires may eventually out perform the state of the art entangled LED[8] since all of the injected current is expected to flow through the quantum dot.

Methods. *Nanowire Growth and Device Fabrication.* The nanowire quantum dots were grown in the vapor−liquid−solid mode[28] by means of metal−organic vapor phase epitaxy (MOVPE) in a similar manner as reported in previous work.[29,30] Colloidal Au particles of 20 nm diameter were used to first grow an InP section for 20 min (~2 μm) followed by 1 s of InAsP growth. The 4 μm long nanowires were completed by another 20 min of InP growth. The dot size for 1 s growth is estimated to be 4−6 nm high and 30−40 nm in diameter based on energy dispersive X-ray analysis in a transmission electron microscopy from previous studies on similar dots.[16] After growth, the InP nanowires were transferred from the InP growth to a prepatterned p^{++} silicon wafer with SiO_2 layer of 285 nm. Individual wires were contacted by e-beam lithography and metal evaporation (100 nm Ti/20 nm Au). Precise positioning of lateral gates to a single nanowire was achieved by overlapping an atomic force microscopy image and design file with the use of four alignment markers. The position of the quantum dot is not precisely known and is assumed to be in the middle of the nanowire based on the reproducibility of MOVPE synthesis growth rates.

Device Characterization. The single quantum dot embedded in nanowire devices was characterized with a standard microphotoluminescence (PL) setup at low temperature (4.2 K). The single quantum dot PL was excited and collected using the same microscope objective with NA = 0.65. The collected PL was dispersed by a single grating spectrometer and collected by a nitrogen cooled Si charge coupled detector with spectral resolution of 30 μeV. Electric field measurements were carried out under low excitation power to observe single excitons and biexcitons with similar emission intensity. To avoid screening effects of the applied lateral electric field on the single quantum dot PL, resonant excitation in the quantum dot d-shell (1.37 eV) was utilized.

AUTHOR INFORMATION

Corresponding Author

*E-mail: m.e.reimer@tudelft.nl.

Author Contributions

§These authors have contributed to this work equally.

ACKNOWLEDGMENT

We acknowledge U. Perinetti and N. Akopian for setup development, M. Hocevar for the SEM image, G. Bulgarini, M. Korkusinski, P. Hawrylak, and R.L. Williams for scientific discussions, and R. N. Schouten for technical assistance. This work was supported by the Dutch ministry of economic affairs (NanoNed DOE7013), the Dutch Organization for Fundamental Research on Matter (FOM), the European FP6 NODE (015783) project, the DARPA QUEST Grant HR0011-09-1-0007, and The Netherlands Organization for Scientific Research (NWO).

REFERENCES

(1) Shields, A. *Nat. Photonics* **2007**, *1*, 215–223.
(2) Gisin, N.; Thew, R. *Nat. Photonics* **2007**, *1*, 165–171.
(3) Benson, O.; Santori, C.; Pelton, M.; Yamamoto, Y. *Phys. Rev. Lett.* **2000**, *84*, 2513–2516.
(4) Akopian, N.; Lindner, N. H.; Poem, E.; Berlatzky, Y.; Avron, J.; Gershoni, D.; Gerar-dot, B. D.; Petroff, P. M. *Phys. Rev. Lett.* **2006**, *96*, No. 130501.
(5) Muller, A.; Fang, F; Lawall, J; Solomon, G. S. *Phys. Rev. Lett.* **2009**, *103*, No. 217402.
(6) Young, R. J.; Stevenson, R. M.; Atkinson, P.; Cooper, K.; Ritchie, D. A.; Shields, A. J. *New J. Phys.* **2006**, *8*, 29.
(7) Hafenbrak, R.; Ulrich, S. M.; Micher, P.; Wang, L.; Rastelli, A.; Schmidt, O. G. *New J. Phys.* **2007**, *9*, 315.
(8) Salter, C. L.; Stevenson, R. M.; Farrer, I.; Nicoll, C. A.; Ritchie, D. A. *Nature (London)* **2010**, *465*, 594–597.
(9) Mohan, A.; Felici, M.; Gallo, P.; Dwir, B.; Rudra, A.; Faist, J.; Kapon, E. *Nat. Photonics* **2010**, *4*, 302–306.
(10) Greilich, A.; Schwab, M.; Berstermann, T.; Auer, T.; Oulton, R.; Yakovlev, D. R.; Bayer, M.; Stavarache, V.; Reuter, D.; Wieck, A. *Phys. Rev. B* **2006**, *73*, No. 045323.
(11) Stevenson, R. M.; Young, R. J.; Atkinson, P.; Cooper, K.; Ritchie, D. A.; Shields, A. J. *Nature (London)* **2006**, *439*, 179–182.
(12) Kowalik, K.; Krebs, O.; Lemaître, A.; Eble, B.; Kudelski, A.; Voisin, P.; Seidl, S.; Gaj, J. A. *Appl. Phys. Lett.* **2007**, *91*, No. 183104.
(13) Gerardot, B. D.; Seidl, S.; Dalgarno, P. A.; Warburton, R. J.; Granados, D.; Garcia, J. M.; Kowalik, K.; Krebs, O.; Karrai, K.; Badolato, A.; Petroff, P. M. *Appl. Phys. Lett.* **2007**, *90*, No. 041101.
(14) Vogel, M. M.; Ulrich, S. M.; Hafenbrak, R.; Michler, P.; Wang, L.; Rastelli, A.; Schmidt, O. G. *Appl. Phys. Lett.* **2007**, *91*, No. 051904.
(15) Singh, R.; Bester, G. *Phys. Rev. Lett.* **2009**, *103*, No. 063601.
(16) van Weert, M. H. M.; Akopian, N.; Perinetti, U.; van Kouwen, M. P.; Algra, R. E.; Ver-heijen, M. A.; Bakkers, E. P. A. M.; Kouwenhoven, L. P.; Zwiller, V. *Nano Lett.* **2009**, *9*, 1989–1993.
(17) Reimer, M. E.; Korkusinski, M.; Lefebvre, J.; Lapointe, J.; Poole, P. J.; Aers, G. C.; Dalacu, D.; McKinnon, W. R.; Frederick, S.; Hawrylak, P.; Williams, R. L. arXiv:0706.1075.
(18) Reimer, M. E.; Korkusiński, M.; Dalacu, D.; Lefebvre, J.; Lapointe, J.; Poole, P. J.; Aers, G. C.; McKinnon, W. R.; Hawrylak, P.; Williams, R. L. *Phys. Rev. B* **2008**, *78*, No. 195301.
(19) Korkusinski, M.; Reimer, M. E.; Williams, R. L.; Hawrylak, P. *Phys. Rev. B* **2009**, *79*, No. 035309.
(20) Avron, J. E.; Bisker, G.; Gershoni, D.; Lindner, N. H.; Meirom, E. A.; Warburton, R. J. *Phys. Rev. Lett.* **2008**, *100*, No. 120501.
(21) Ding, F.; Singh, R.; Plumhof, J. D.; Zander, T.; Křápek, V.; Chen, Y. H.; Benyoucef, M.; Zwiller, V.; Dörr, K.; Bester, G.; Rastelli, A.; Schmidt, O. G. *Phys. Rev. Lett.* **2010**, *104*, No. 067405.

(22) Reimer, M. E.; Dalacu, D.; Poole, P. J.; Williams, R. L. *J. Phys.: Conf. Ser.* **2010**, *210*, No. 012019.
(23) van Kouwen, M. P.; Reimer, M. E.; Hidma, A. W.; van Weert, M. H. M.; Algra, R. E.; Bakkers, E. P. A. M.; Kouwenhoven, L. P.; Zwiller, V. *Nano Lett.* **2010**, *10*, 1817–1822.
(24) Baier, M.; Findeis, F.; Zrenner, A.; Bichler, M.; Abstreiter, G. *Phys. Rev. B* **2001**, *64*, No. 195326.
(25) van Weert, M. H. M.; Akopian, N.; Kelkensberg, F.; Perinetti, U.; van Kouwen, M. P.; Ri-vas, J. G.; Borgström, M. T.; Algra, R. E.; Verheijen, M. A.; Bakkers, E. P. A. M.; Kouwen-hoven, L. P.; Zwiller, V. *Small* **2009**, *5*, 2134–2138.
(26) Kaniber, M.; Huckand, M. F.; Müller, K.; Clark, E. C.; Troiani, F.; Bichler, M.; Krenner, H. J.; Finley, J. J. arXiv:1009.1989.
(27) Claudon, J.; Bleuse, J.; Malik, N. S.; Bazin, M.; Jaffrennou, P.; Gregersen, N.; Sauvan, C.; Lalanne, P.; Gerard, J.-M. *Nat. Photonics* **2010**, *4*, 174–177.
(28) Wagner, R.; Ellis, W. *Appl. Phys. Lett.* **1964**, *4*, 89.
(29) Minot, E. D.; Kelkensberg, F.; van Kouwen, M.; van Dam, J. A.; Kouwenhoven, L. P.; Zwiller, V.; Borgström, M. T.; Wunnicke, O.; Verheijen, M. A.; Bakkers, E. P. A. M. *Nano Lett.* **2007**, *7*, 367–371.
(30) van Kouwen, M. P.; van Weert, M. H. M.; Reimer, M. E.; Akopian, N.; Perinetti, U.; Al-gra, R. E.; Bakkers, E. P. A. M.; Kouwenhoven, L. P.; Zwiller, V. *Appl. Phys. Lett.* **2010**, *97*, No. 113108.

■ NOTE ADDED AFTER ASAP PUBLICATION

This paper published ASAP January 12, 2011 with errors in the TOC artwork, Figure 4, and throughout the text. The correct version published February 9, 2011.